

CEBAF Program Advisory Committee Six (PAC6) Proposal Cover Sheet

This proposal must be received by close of business on April 5, 1993 at:

CEBAF
User Liaison Office
12000 Jefferson Avenue
Newport News, VA 23606

Proposal Title

Measurement of Single Pion Electroproduction from the Proton with Polarized Beam and Polarized Target Using CLAS

Contact Person

Name: Dr. Henry Weller

Institution: Duke University and Triangle Universities Nuclear Laboratory

Address: Science Drive; Box 90308

Address:

City, State ZIP/Country: Durham, NC 27708-0308

Phone: 919/660-2633

FAX: 919/660-2525

E-Mail → BITnet:

Internet: WELLER@TUNL.TUNL.DUKE.EDU

If this proposal is based on a previously submitted proposal or letter-of-intent, give the number, title and date:

CEBAF Use Only

Receipt Date: 4/5/93 Log Number Assigned: PR 93-036

By: go

**Measurement of Single Pion Electroproduction
from the Proton with Polarized Beam and
Polarized Target Using CLAS**

Spokespersons: H. Weller, R. Chasteler, R. Minehart

The N^* Group in the CLAS Collaboration

V. Burkert, D. Joyce, B. Mecking, B. Niczyporuk,
E. Smith, A. Yegneswaran
CEBAF, Newport News, Virginia

R. Chasteler, H. Weller
Duke University, Durham, North Carolina

D. Crabb, D. Day, R. Marshall, J. McCarthy, R. Minehart
O. Rondon-Aramayo, R. Sealock, L.C. Smith, S. Thornton, H.J. Weber
University of Virginia, Charlottesville, Virginia

P. Stoler, G. Adams, N. Mukhopadyay
Rensselaer Polytechnic Institute, Troy, New York

K. Beard, C. Carlson, H. Funsten
College of William and Mary, Williamsburg, Virginia

D. Isenhower, M. Sadler
Abilene Christian University, Abilene, Texas

D. Doughty, D. Heddle, Z. Li
Christopher Newport University, Newport News, Virginia

L. Dennis, A. Tam
Florida State University, Tallahassee, Florida

S. Dytman, T. Donoghue
University of Pittsburg, Pittsburg, Pennsylvania

J. Lieb
George Mason University, Fairfax, Virginia

K. Giovanetti
James Madison University, Harrisonburg, Virginia

M. Manley
Kent State University, Kent, Ohio

C. Stronach
Virginia State University, Petersburg, Virginia

M. Gai
Yale University, New Haven, Connecticut

Abstract

An extensive study of the structure of the nucleon and its excited states is planned for the CLAS detector at CEBAF. The N* group has proposed experiments using unpolarized hydrogen and deuterium targets to measure the electromagnetic transition form factors to the nucleon resonances. These form factors are dependent on the spin of the electron and the target nucleon, so that a complete model-independent determination requires measurements with polarized electrons and polarized nucleons. An experiment to study the inclusive scattering of polarized electrons on the protons in a polarized solid state $^{15}\text{NH}_3$ target in the CLAS has already been approved (Proposal 91-023). We propose a concurrent experiment, requiring no new beam time allocation, to measure single pion production in the reactions,

$$\vec{e} + \vec{p} \rightarrow e' + \pi^+ + n.$$

and

$$\vec{e} + \vec{p} \rightarrow e' + \pi^0 + p.$$

Three independent asymmetry ratios can be obtained in bins in a four dimensional parameter space, (Q^2, W, θ, ϕ) , free of uncertainties associated with the CLAS acceptance. This will be the first measurement of spin asymmetries for exclusive pion production in the nucleon resonance region. It is anticipated that this first experiment will lead to statistically useful results and will point the way to further experiments at the CLAS.

In this proposal we present estimates of the expected order of magnitude of the asymmetries using the AO computer program developed at CEBAF and an approximate treatment of the acceptance function for the CLAS detector with a polarized target installed. We show that the proposed experiment will provide asymmetry measurements over a large range of Q^2 and W with significant statistical precision. We show, using models for the resonance region with parameters chosen to fit existing experimental cross sections, that the expected asymmetries can be large. We also show sensitivity to the details of models of the baryon structure by calculations made with different assumptions about the nature of the Roper resonance, chosen because it has a small amplitude for electroproduction and may have an important interpretation in terms of gluonic excitations of the nucleon. We also show the effect of removing various resonance amplitudes from the model calculation.

We emphasize that this is primarily a discovery measurement to determine the order of magnitude and functional dependence of the heretofore unmeasured asymmetries, and to determine how well the CLAS with a polarized target is suited to their determination.

I. Introduction

The study of the hadronic structure of baryons at CEBAF will be significantly enhanced through the use of a polarized electron beam and polarized targets. For electro-production of single mesons by polarized electrons on polarized nucleons there are six complex helicity amplitudes associated with the γNN^* vertex, illustrated in Figure 1. These amplitudes are functions of the momentum transfer Q^2 , the resonance mass, W , and the decay angle of the pion, θ_π , measured relative to \vec{q} in the rest frame of the resonance. The cross section consists of bilinear combinations of these amplitudes and kinematical factors depending on the angle ϕ , the longitudinal-transverse polarization parameter ϵ , and the angle between \vec{q} and the target polarization. For this experiment, the target and the beam are both polarized along the beam direction so that this latter angle is simply the angle between \vec{q} and the beam, θ_γ .

The cross section can be written in the form:

$$\sigma = \sigma_0 + P_e \sigma_e + P_p \sigma_p + P_e P_p \sigma_{ep} \quad (1)$$

where σ_0 is the unpolarized cross section, σ_e , σ_p , and σ_{ep} are additional terms depending on the beam and target polarization. The quantity P_e is the longitudinal beam polarization, and P_p is the longitudinal polarization of the target proton. The explicit representation of each cross section in terms of the helicity amplitudes is given in the Appendix. A measurement with unpolarized beam and target can determine only σ_0 . With a polarized beam, we can also determine σ_e , which is expected to be small. Measurement of σ_p , which model calculations indicate will be larger, requires a polarized target. Measurement of the double polarization term, σ_{ep} , requires both polarized beam and target.

In an ideal experiment, each cross section would be measured absolutely at every point in the accessible parameter space. For each choice of Q^2 , measurements at different incident beam energies and over the full angular range of the decay pion permit the separation of each individual cross section into a number of independent bi-linear combinations of helicity amplitudes. However, uncertainties in the acceptance function for the detector will make meaningful extraction unlikely. We propose instead to measure the following asymmetries at each point in the parameter space:

$$A_e = \frac{N(++)+N(+)-N(-+)-N(--)}{N(++)+N(+)+N(-+)+N(--)} = P_e \frac{\sigma_e}{\sigma_0} \quad (2)$$

$$A_p = \frac{N(++)-N(+)-N(-)+N(--)}{N(++)+N(+)+N(-)+N(--)} = P_p \frac{\sigma_p}{\sigma_0} \quad (3)$$

$$A_{ep} = \frac{N(++)-N(+)-N(-)+N(--)}{N(++)+N(+)+N(-)+N(--)} = P_e P_p \frac{\sigma_{ep}}{\sigma_0} \quad (4)$$

where the first sign in $N(++)$ specifies the electron helicity and the second specifies the proton helicity, both relative to the incident electron beam. In these ratios the acceptance function cancels. This cancellation is purchased at the price of measuring ratios of complicated linear sums of bilinear products of the helicity amplitudes.

To first order any measurement of these asymmetries provides new data never before measured. Analyses based on the present world data base, which contains no data for pion production with polarization, predicts non-zero values for the asymmetries. That fact alone tells us that the amplitudes derived from fits to data are already sensitive to the polarization measurements. To further quantify the sensitivity we have calculated asymmetries using the ‘‘Amplitudes and Observables’’ program, AO, developed at CEBAF [AO]. We have studied the effect of varying some of the resonance amplitudes by setting them individually to zero, or, as in the case of the Roper amplitudes, by choosing them according to various models.

As discussed in the proposal for inclusive electron scattering, CLAS is well matched for polarized target experiments both in terms of luminosity and in the structure of its magnetic field. Only moderate luminosity can be achieved both for polarized solid state targets [MEY85,WPT84], and for polarized gas targets. The maximum luminosity is limited to about $\simeq 5 \times 10^{34} \text{ cm}^{-2} \text{ sec}^{-1}$ for radiation resistant ammonia targets (the luminosity is given in terms of the total number of nucleons in the target including the nitrogen host material). This limit is well matched to the expected luminosity limitation of the CLAS. The low luminosity is compensated by the large acceptance of the CLAS detector so that reasonable count rates can be achieved with these targets. The operation of the target is not disturbed by the CLAS magnet due to the fact that the on-axis field of CLAS is nearly zero. The 5 Tesla holding field associated with the hydrogen polarized target does deflect both the electron beam and the reaction products significantly, but the particle trajectories can be reconstructed to retrieve the kinematic quantities of interest.

To estimate the asymmetries and the errors for the proposed measurements we used a simulation program to calculate the acceptance of the CLAS for single pion production with the polarizing target magnet in place. Electrons will be detected in the forward calorimeter ($10^\circ - 45^\circ$). The CLAS magnet will deflect the scattered electrons towards the beam axis. The strength of the field varied from 1/3 full-field at the lowest energy to 2/3 full-field at the highest energy. The pion (or the proton, depending on the reaction) laboratory angle with respect to the beam was required to be less than 50° in order to miss the polarized target magnet coil. Both the electrons and hadrons were required to miss the CLAS toroid coils. The acceptance was calculated for a variety of Q^2 , W , θ and ϕ (see Figure 1 for the definition of the angles) at the incident energies of proposal (91-023). The large size of the parameter space makes it difficult to show these results in detail. Typical ones are shown in Fig. 2. For this example the acceptance at the order of 40% for π^0 production is determined primarily by the acceptance of the scattered electron. For π^+ production, the acceptance is somewhat smaller. The difference is due to the fact that in the former case we detect the proton, which is confined to directions in a small cone around \vec{q} , while in the latter we detect the π^+ which is not restricted in direction. Other features of the acceptance that can be noted is that at $E_0 = 2.4\text{GeV}$ we can study the range, $.25 < Q^2 < 1.75$, while at $E_0 = 4.0\text{GeV}$, the electron acceptance is limited to $Q^2 > 0.7\text{GeV}$. The details of these limits are determined by the choice of the magnetic field, which will be constrained by the requirements of Exp. (91-023).

We used the AO program developed at CEBAF to calculate the cross sections, asymmetries and statistical errors, assuming the energies, luminosities and running times planned for Exp. (91-023) and shown in Table 1.

Table 1: CLAS Operating Conditions for Proposal 91-023		
Energy (MeV)	Luminosity ($cm^{-2}sec^{-1}$)	Run Time (hours)
1200	$2 \cdot 10^{33}$	150
1600	$2 \cdot 10^{33}$	150
2000	$3 \cdot 10^{33}$	150
2400	$5 \cdot 10^{33}$	150
2800	$5 \cdot 10^{33}$	200
3200	$1 \cdot 10^{34}$	200
4000	$1 \cdot 10^{34}$	200

In our analysis we have assumed that all six sectors of the CLAS are instrumented. The values of the electron and proton polarizations were taken to be $P_e = 0.5$, and $P_p = 0.9$. respectively. As discussed in the proposal for Exp. (91-023) the choice of P_e is rather conservative, in view of recent advances in the development of strained GaAs polarized electron sources capable of producing electron beams with currents of 15-30 μA with polarization in excess of 0.75 [CAR91]. The choice of P_p is consistent with recent results. A proton polarization of 0.96 was achieved[CRA90a] using irradiated $^{15}NH_3$ as a target material in a 5T magnetic field at 1 K.

With $^{15}NH_3$ as a polarized target material, the high resolution that will be obtained with the CLAS means that the effective polarization in exclusive scattering is given by the polarization of the protons themselves. The nitrogen provides a background that limits the luminosity but it produces only a small dilution factor, since with the high resolution provided by the CLAS detector exclusive reactions on bound protons can be separated from those on free protons with a background from quasi-free production on the protons in the nitrogen. This background contributes very little to the differences in the numerator of the asymmetry, but it adds to the total cross section in the denominator.

Calculations of missing mass plots have been performed at CEBAF by Bogdan Niczyporuk for pion production on $^{15}\text{NH}_3$. In this plot the unshaded portion represents elastic scattering from hydrogen plus quasielastic scattering from ^{15}N (no pion production). The shaded area represents all inelastic scattering processes. The unshaded area includes the shaded, so the top of the histogram gives the total response. The results (see Fig. 3) indicate that we can clearly resolve the elastic scattering from pion production and furthermore that the background due to ^{15}N is rather small. We estimate that subtraction of the background will increase the error in our asymmetry measurements by about a factor of 1.25 in the worst case. This effect is not included in the figures given in this proposal. An increase of P_e from 0.5 to 0.75 (which seems to be quite likely for the beam currents of this experiment), will compensate for the increase in error introduced by the nitrogen.

In Fig. 4, we show some typical estimated errors for the asymmetry measurements as a function of $\cos\theta$ for W in the mid-range of the resonance region and for $Q^2 = 0.5(\text{GeV}/c)^2$. For this calculation the bin sizes(Full width) were taken to be: $\Delta Q^2 = 0.2Q^2$, $\Delta W = 20 \text{ MeV}$, $\Delta \cos\theta = 0.1$, and $\Delta\phi = 18^\circ$. This choice of bin size is somewhat arbitrary, but it is desirable to make it small enough to see structure in the resonance region. Eventually, a combined analysis of cross sections and asymmetries will have to fit the data over a large parameter space with a limited number of fitting coefficients, so that the effective errors are actually much smaller than shown in the figure. We will illustrate this in the following section by considering asymmetry measurements multiplied by various combinations of $\cos\theta$, $\sin\phi$, and $\cos\phi$, and integrated over the θ and ϕ part of the parameter space. To provide a specific example for the sake of discussion, we will present results of calculations showing the effect of various models of the Roper on the asymmetries. The results are discussed in the next section.

II. Sensitivity to Models of the Roper resonance.

In the non-relativistic quark model (NRQM) the lowest mass $P_{11}(1440)$ state, usually called the Roper, is assigned to a radially excited 3-Quark state $[q^3]$ within the $\text{SU}(6)\times\text{O}(3)$ super-multiplet $[56, 0^+]_2$ (i.e. $L_{3Q} = 0$, $N_{3Q} = 2$). However, the observed low mass of the state, as well as the sign and magnitude of the photocoupling amplitudes have been difficult to reproduce within the

framework of the NRQM. Moreover, there is experimental evidence that the Q^2 dependence of the photocoupling amplitude $A_{1/2}(Q^2)$ may be quite different from what is predicted in the NRQM framework [LIB91]. The predictions of several different models, along with the small amount of existing data, are shown in Figure 5. The data indicate a rapid fall-off of this amplitude with Q^2 whereas the NRQM and the relativized versions predict a much weaker fall-off or even a rise with Q^2 . However, the experimental information about electroproduction amplitudes of the Roper is rather limited, largely due to the complete lack of polarization data, and definite conclusions about the nature of the Roper cannot be drawn from existing data.

Recently, there have been theoretical speculations [LIZ91] that the Roper resonance might not be a regular $[q^3]$ state, but the hybrid ($[q^3G]$, 3-quarks with one valence gluon) equivalent of the nucleon.

Obviously, the solution to the puzzle of the structure of the $P_{11}(1440)$ could have enormous impact on our understanding of baryon structure and the dynamics of the strong interaction in the non-perturbative regime. It has been pointed out [LIB91] that a precise measurement of the Q^2 dependence of the $\gamma_v p P_{11}(1440)$ transition form factor provides a unique means of discriminating between the interpretation of the Roper as a regular $[56, 0^+]_2 [q^3]$ state, or as a hybrid $[70, 0^+]_0 [q^3G]$ state. The discriminating power results from the different spin-flavor factors in the respective photocoupling amplitudes, such that in the first approximation:

$$\frac{A_{1/2}(P_{11}(1440))[70, 0^+]_0}{A_{1/2}(P_{11}(1440))[56, 0^+]_2} \sim \frac{1}{Q^2} \quad (4)$$

Therefore, the Roper is likely to fall off much more rapidly with Q^2 if it is a hybrid state than if it is a regular 3-quark state. Measurement of the Q^2 dependence of the Roper photocoupling amplitude can thus be used to discriminate between various spectroscopic assignments. The calculation based on the hybrid interpretation is in better agreement with the data than calculations using the non-relativistic or relativized versions of the constituent quark model (Figure 5).

One of the objectives of the inclusive polarized $e + p$ experiment (91-023) is to determine the polarization structure function A_1 for inelastic electron scattering. A_1 is directly related to the differences in the total transverse absorption

cross section for helicity 1/2 and 3/2:

$$A_1 = \frac{\sigma_{1/2}^T - \sigma_{3/2}^T}{\sigma_{1/2}^T + \sigma_{3/2}^T}$$

Calculations of A_1 using both the 3-quark model [q^3] and the hybrid model [q^3G] have been performed and are shown in Fig. 6, along with the expected errors for the data of (91-023). Substantial differences are seen, especially at high values of Q^2 .

We believe that the sensitivity of the exclusive pion-channels to the details of the specific models for the various excited states of the nucleon will provide a wealth of information. We shall illustrate this with several calculations of some of the observables of the present proposal, performed using the AO computer code.

The following two figures (7 and 8) display some representative results of calculations showing the sensitivity of the asymmetries for π^+ and π^0 electro-production, respectively, to the choice of the theoretical model for the Roper resonance ($P_{11}(1440)$). Results are shown for a “low” and a “high” value of Q^2 , for the polarized target asymmetry only. Since the asymmetries can be expanded in terms of products of Legendre polynomials and $\sin n\phi$, we can utilize the orthogonality of these functions, multiply by one of them and obtain an “expansion coefficient”. This is a somewhat arbitrary but simple way of looking at specific angle (non-integrated) dependent features of the asymmetries. Two selected coefficients, chosen because they displayed large effects, are shown in Figs. 7 and 8. No background terms were used since they had no effect on the calculated asymmetries. The plots contain:

AO fit: uses the measured branching ratios for pion production from experiment and resonance amplitudes fitted to existing data, along with models for weak amplitudes. Born terms are included.

Hybrid Roper : uses the experimental parameters for all resonances (as in the AO fit) except for the Roper resonance, which is treated as a hybrid state as defined by Li and Burkert [LIB91]. Born terms are included.

No Roper : uses the experimental parameters for all resonances except for the Roper resonance, which is turned off. Born terms are included.

Li-Close: uses the experimental parameters for all resonances except for the Roper resonance, for which the Li-Close [CLO90] is used. Born terms are included.

The electron polarization was taken to be 0.5, and the proton (target) polarization was taken to be 0.9. Count rates are based on a Q^2 bin-size of $0.2Q^2$ (full width), and a bin size of 0.02 GeV for the resonance mass, W . Steps of 0.1 in $\cos\theta$ and 10° in ϕ were used. The acceptance restrictions due to target coils and the CLAS toroid have been included as previously described.

It should be emphasized that there are no experimental data for any of these observables. The data points of Figs. 7 and 8 are creations of the AO code, and are based on previous unpolarized measurements of pion electroproduction cross sections. Note that the Roper resonance has not been observed unequivocally in unpolarized electroproduction data (only in photoproduction data). The error bars are the most significant aspect of the data points in Figs. 7 and 8, since they reflect the anticipated uncertainty we expect on the basis of the running times of (91-023).

The results shown in Figs. 7 and 8 indicate that the polarized target asymmetries are sensitive not only to the difference between the Hybrid Roper and the $[q^3]$ (Li-Clouse) Roper, but also to the difference between the Hybrid Roper and No-Roper models. It can be seen that this latter difference gets much smaller at the higher values of Q^2 , as expected from eq. 4.

III. Sensitivity of π^+ Electroproduction Asymmetries to Other Resonances

Figure 9 is presented in order to give an indication of the sensitivity of the polarized target asymmetries for π^+ electroproduction to the presence of a few other baryon resonances. In this case the asymmetry A_t has been integrated over all values of θ , and ϕ from 0° -to- 180° . Of course, much more information is available in the non-integrated values of A_t . The AO fit is the same as in the previous figures. The four other curves are what was calculated when the corresponding resonance was turned off. Sizeable effects are seen, for example, at 4.0 GeV and $Q^2 = 0.75 \text{ GeV}^2$ when either the $D_{13}(1520)$ or the $P_{33}(1232)$ resonance is turned on and/or off. Further work will be done to see if differences corresponding to small changes in these amplitudes are observable.

Finally, we mention that what we would most like to demonstrate is how the asymmetries would serve to eliminate ambiguities in a model-independent

extraction of helicity amplitudes from data. A program to do this does not exist, but plans for creating one (or at least one with a minimal amount of model dependence) are under-way at CEBAF. Intuitively, we expect that the asymmetry measurements will play an important role.

IV. Experimental Considerations

Most of the relevant experimental considerations have been discussed in proposal (91-023), and we will adhere to their procedures and considerations. A few salient aspects of the experiment will be mentioned here.

Electron Polarization:

The electron polarization will be measured with the Möller polarimeter presently under construction (R. Chasteler) for Hall B. At 2 GeV (for example), 3% statistical accuracy can be obtained in 25 seconds. The polarimeter design is shown in Fig. 10, while the running times for 3% accuracy are given in Fig. 11.

Target Polarization:

Direct measurement (NMR) has an absolute accuracy of about 3%. The unpaired proton in ^{15}N will also be polarized. With dilution considered, this is a contribution of about 6% of the free proton polarization. This can be calculated to about 30% accuracy using good ^{15}N wavefunction, leaving a systematic error less than 2% (refer to proposal 91-023).

As proposed in (91-023), a second determination of the product of beam and target polarization will also be employed. Measurement of the asymmetry for elastic scattering and (separated by CLAS) quasi-elastic scattering from the bound protons (using an ^{15}N target) allows a determination of the product of the polarizations if done at small Q^2 where G_E^P and G_M^P are known. An accurate electron polarization measurement (above) will allow the separation of this product, which is needed for the proposed asymmetry measurements.

Background from quasi-free production on ^{15}N :

The protons in nitrogen are only weakly polarized and will contribute only a small effect to the difference used in the numerator of the asymmetry. However the denominator is the unpolarized cross section. The CLAS resolution will be

good enough for the missing mass plot to consist of a narrow peak from free protons riding on a much broader peak from the bound protons (broadened by Fermi motion). The ratio of free to bound protons is 3:7, but the Fermi motion is expected to make the signal to background ratio more like 2:1. This will increase the error bars in each bin by about 25%, as previously described (Fig.3).

Beam Handling:

To avoid local depolarization or polarization buildup, the incident beam will be rastered across the front face of the target. High speed rastering is necessary to avoid local temperature rises. Four small dipole magnets will be located upstream in the beam line for this purpose.

Background and Luminosity:

Simulations with the Geant3 program indicate that the longitudinal field of the target acts like a focussing lens if the target is polarized along the beam direction. This shields the CLAS detectors from low energy particles. There is no apparent effect on the wire chambers (Ref. 91-023). We expect to achieve typical luminosities of 10^{34} cm² s⁻¹ in the proposed experiment.

CLAS Performance with Polarized Target Field:

As discussed in Proposal (91-023), the polarized target field of 5T results in $\int Bdl = 1.0Tm$. Trajectories have been traced with GEANT, showing a cut-off at 150 MeV/c, and a shift in the ϕ angle. The momentum resolution is not affected since most of the polarized target field is not in the region where the tracking is done.

V. Summary of Beam Requests and Equipment Requirements

For this proposal our request for running time, beam energies, approximate currents, and targets is identical to that already assigned to Exp. 91-023. The breakdown of this time into the various energies and targets is summarized in Table 2. The quoted numbers do not include time needed for servicing the polarized target. All measurements will be conducted using the polarized electron source. In our simulations we assumed that the CLAS detector will be fully instrumented with tracking chambers, gas Cerenkov counters, scintillation counters, and electromagnetic calorimeters for angles up to 45°. Significant reductions from these assumptions will probably make it difficult to derive anything other than upper limits on the asymmetry functions. The statistical error

achieved is proportional to $1/P_e$, so that the anticipated improvement in the electron polarization from 0.5-to-0.75 is extremely valuable.

VI. Responsibilities

As stated in the proposal (91-023) CEBAF and the University of Virginia are jointly responsible for the construction and operation of the polarized target magnet, and the target cryostat. The data will be analyzed jointly by various members of the collaboration, with the Duke University group and the U.Va. group taking responsibility for the extraction of the pion production asymmetry ratios.

Table 2: CEBAF Operating Conditions for Proposal 91-023			
Energy (MeV)	Target	Current (nA)	Running Time (hours)
1200	$^{15}\text{NH}_3$	1	150
1200	^{15}N	1	15
1600	$^{15}\text{NH}_3$	1	150
1600	^{15}N	1	15
2000	$^{15}\text{NH}_3$	1.5	150
2000	^{15}N	1.5	15
2400	$^{15}\text{NH}_3$	2.5	150
2400	^{15}N	2.5	15
2800	$^{15}\text{NH}_3$	2.5	200
2800	^{15}N	2.5	20
3200	$^{15}\text{NH}_3$	5	200
3200	^{15}N	5	20
4000	$^{15}\text{NH}_3$	5	200
4000	^{15}N	5	20
TOTAL	$^{15}\text{NH}_3$		1,200
TOTAL	^{15}N		120

Summary

Asymmetry data for the exclusive reactions

$$\vec{e} + \vec{p} \rightarrow e' + \pi^+ + n.$$

and

$$\vec{e} + \vec{p} \rightarrow e' + \pi^0 + p.$$

will be obtained for the first time. Three asymmetries, A_e , A_t and A_{et} will be measured as a function of beam energy from 1.2 to 4.0 GeV, for Q^2 from 0.25 to 1.25 GeV². These asymmetries, which arise from interference between various helicity amplitudes, will be especially sensitive to small effects in these amplitudes. As an illustration of this we have calculated the asymmetries for two different models of the Roper resonance. The results show a strong sensitivity to the $[q^3]$ vs. the $[q^3G]$ model of the Roper, even in the angle integrated asymmetries. Much greater detail and sensitivity is expected in the differential quantities. Preliminary studies also show that the asymmetries are sensitive to the presence of other resonances.

No new beam time is requested for this experiment. The results obtained here should be of great value in planning future studies of these reactions using the polarized beam, polarized target, and the CLAS.

References

- [AO] V. Burkert, *et al.*, CEBAF Computer Program.
- [BOD] B. Boden and G. Kroesen, Research Program at CEBAF II, Report of the 1986 Summer Study Group, eds. V. Burkert *et al.*, Newport News, VA 23606, USA, and private communications.
- [CLO90] Z.P. Li and F.E. Close, *Phys. Rev.* **D42**, 2207 (1990), and R. Kuniuk and N. Isgur, *Phys. Rev.* **D21**, 1888 (1980).
- [CRA90a] D. G. Crabb *et. al.*, *Phys. Rev. Lett.* **64**, 2627 (1990).
- [CRA90b] D. G. Crabb; Talk presented at the Workshop on Polarized Solid Target, Bonn, Germany, 7-8 Sept. 1990.
- [FOS82] F. Foster and G. Hughes, *Z. Phys.* **C14**, 123 (1982).
- [GER80] C. Gerhardt, *Z. Phys* **C4**, 311 (1980).
- [LIB91] Z.P. Li, V. Burkert, Z. Li; *Phys. Rev.* **D46**, 72 (1992).
- [LIZ91] Z.P. Li; *Phys. Rev.* **D44**, 2841 (1991).
- [MEY85] W. Meyer; 1985 CEBAF Summer Workshop, pg 237.
- [WEB90] H.J. Weber, *Phys. Rev.* **C41**, 2783 (1990).
- [WPT84] Proceedings 4th International Workshop on Polarized Target Materials and Techniques, Bad Honnef, September 1984.

Figure Captions

Figure 1. A diagram of the $p(e,e')\pi N$ reaction. In this example the production of a resonance decaying into a nucleon and a pion is assumed. \vec{q} makes an angle θ_γ with respect to the initial electron beam. The angles θ_π (θ_N) and ϕ specify the direction of the outgoing pion (nucleon).

Figure 2. The acceptance of CLAS for π° production using the $\bar{p}(\vec{e}, e')p\pi^\circ$ reaction with a polarized $^{15}\text{NH}_3$ target as a function of $\cos\theta_\pi$ (see Fig. 1) for $Q^2 = 0.5(\text{Gev}/c)^2$ and $W = 1.44$ GeV.

Figure 3. Missing mass calculation (performed by B.Niczyporuk using the SDA program) for the $e^- + ^{15}\text{NH}_3 \rightarrow e^- + p + \pi^\circ$ reaction at 2.4 GeV. The unshaded area represents events associated with elastic scattering in hydrogen and quasielastic scattering in ^{15}N . The shaded area represents all inelastic events, including pion production. The contribution of the Nitrogen can be seen by comparing to the upper graph which is the same calculation for the $e^- + p \rightarrow e^- + p + \pi^\circ$ reaction. Note that the pions are nicely resolved and that the Nitrogen induced background is quite small.

Figure 4. The error in the asymmetry A_t for π° production in the $\bar{p}(\vec{e}, e')p\pi^\circ$ reaction at $E = 2.4$ GeV, $Q^2 = 0.50$ (GeV/c) 2 and $W = 1.45$ GeV, as a function of the cosine of the pion angle θ_π (see Fig. 1). The acceptance calculation is described in the text.

Figure 5. $A_{1/2}^P(Q^2)$ for the transition $\gamma_\nu p \rightarrow P_{11}$ if the Roper is a q^3 state [CLO90] (long-dashed line), or a q^3G state (solid line), respectively. The short-dashed and the dash-dotted lines represent different results of the analysis by Gerhardt. Note that the analysis was constrained by fixing the amplitude at the photoproduction point. The data points indicate the results of fits at fixed

Q^2 . Gerhardt, diamond symbols; Boden and Krösen, cross symbols.

Figure 6. Calculations of $A_1(Q^2, W)$ at $Q^2 = 0.25 \text{ GeV}^2$ and $Q^2 = 0.75 \text{ GeV}^2$ using the program described in the text. The ratio σ_L/σ_T was fixed at 0.15. The dashed line shows the result with the assumption that the Roper is a q^3 state and the solid line shows the result if it is assumed to be a hybrid q^3G state. The Roper width was taken to be $\Gamma = 150 \text{ MeV}$. The error bars show the expected measurement errors in $A_1(Q^2, W)$ for the proposed experiment.

Figure 7. The asymmetry A_t (integrated as shown) as a function of W at low and high values of Q^2 for the π^0 channel. The “data points” were manufactured by the AO code using previous unpolarized data. The error bars represent the statistical uncertainties expected in the proposed experiment. The dashed curves use the experimental parameters for all resonances except for the Roper resonance where the Li-Clouse [q^3] model [CLO90] is used. Born terms are also included. The solid curve is the same, but with the Roper resonance deleted. The dotted curve is also the same, except that the Hybrid model [LIZ91] of the Roper resonance [q^3G] is used.

Figure 8. Same as Fig. 7, but for the π^+ channel.

Figure 9. The integrated asymmetry A_t for the $\bar{p}(\bar{e}, e')\pi^+n$ reaction at 4.0 GeV and various values of Q^2 . The data were constructed by the AAO code using the results of previous unpolarized measurements. The various curves correspond to deleting the denoted resonance from the calculation.

Figure 10. The TUNL designed Double-Quadrupole Möller Polarimeter for Hall B. This design allows use of one target in one position for beam energies from 0.7 to 6.0 GeV.

Figure 11. Table showing running times needed to obtain 3% statistical errors

in the beam polarization. These are based on a previous one-quadrupole design and will be updated to the new design.

Appendix I - Cross sections in terms of Helicity Amplitudes

The differential cross section can be written as:

$$\sigma = \sigma_0 + \sigma_e + \sigma_p + \sigma_{ep}$$

where the unpolarized cross section is

$$\sigma_0 = \sigma_U + \epsilon\sigma_L + \sqrt{\frac{\epsilon(1+\epsilon)}{2}}\sigma_I \cos \phi + \epsilon\sigma_T \cos(2\phi) = d_0 + d_1 \cos \phi + d_2 \cos(2\phi)$$

In terms of complex helicity amplitudes $H_1 \cdots H_6$,

$$\sigma_U = \frac{1}{2}F \left[|H_1|^2 + |H_2|^2 + |H_3|^2 + |H_4|^2 \right] \quad \sigma_L = F \left[|H_5|^2 + |H_6|^2 \right]$$

$$\sigma_T = F \Re \left(H_2 H_3^* - H_1 H_4^* \right)$$

$$\sigma_I = \frac{F}{\sqrt{2}} \Re \left(H_5 H_4^* - H_5 H_1^* + H_6 H_2^* + H_6 H_3^* \right)$$

$$\sigma_T = F \Re \left(H_2 H_3^* - H_1 H_4^* \right)$$

The polarization cross sections are

$$\sigma_e = s_0 \sin \phi = -F \frac{P_e}{\sqrt{2}} \sqrt{2\epsilon(1-\epsilon)} \Im \left(H_5 H_6^* - H_5 H_1^* + H_6 H_2^* + H_6 H_3^* \right) \sin \phi$$

$$\sigma_p = p_1 \sin \phi + p_2 \sin 2\phi + p_3 \sin 3\phi$$

where

$$p_1 = -FP_p \left[\sin \theta_\gamma \Im (H_4 H_3^* - H_1 H_2^*) + \epsilon \sin \theta_\gamma \left(2H_5 H_6^* + H_2 H_4^* \right) - \sqrt{\epsilon(1+\epsilon)} \cos \theta_\gamma (H_5 H_3^* + H_5 H_2^* - H_6 H_4^* + H_6 H_1^*) \right]$$

$$p_2 = -FP_p \left[\sqrt{\epsilon(1+\epsilon)} \sin \theta_\gamma \Im (H_5 H_3^* + H_6 H_1^*) - \epsilon \cos \theta_\gamma (H_4 H_1 + H_3 H_2) \right]$$

$$p_3 = -FP_p \epsilon \sin \theta_\gamma \Im (H_3 H_1^*)$$

$$\sigma_{ep} = q_0 + q_1 \cos \phi + q_2 \cos 2\phi$$

where

$$q_0 = FP_e P_p \left[\frac{1}{2} \sqrt{1-\epsilon^2} \cos \theta_\gamma (|H_1|^2 - |H_2|^2 - |H_3|^2 + |H_4|^2) + 2\sqrt{\epsilon(1-\epsilon)} \sin \theta_\gamma \Re (H_5 H_2^* - H_6 H_4^*) \right]$$

$$q_1 = -FP_e P_p \left[\sqrt{1-\epsilon^2} \sin \theta_\gamma \Re (H_2 H_1^* + H_3 H_4^*) + \sqrt{\epsilon(1-\epsilon)} \cos \theta_\gamma \Re (H_5 H_3^* + H_5 H_2^* - H_6 H_4^* + H_6 H_1^*) \right]$$

$$q_2 = -FP_e P_p \frac{\sqrt{1-\epsilon^2}}{2} \sin \theta_\gamma \sqrt{2} \Re(H_5 H_3^* + H_6 H_1^*)$$

In the above expressions we have used a kinematical factor:

$$F = \frac{|\vec{p}_\pi| W}{K_L M_p}$$

where

\vec{p}_π is the pion momentum in the center of mass frame of the resonance.

W is the total energy in the center of mass frame of the resonance

M_p is the proton mass,

K_L is the equivalent photon energy in the laboratory frame.

The electron polarization parameter is

$$\epsilon^{-1} = 1 + 2(1 + \nu^2/Q^2) \tan^2(\theta_e/2)$$

The complex helicity amplitudes are functions of Q^2 , W , and θ . The theoretical asymmetries are given by

$$A_e = \sigma_e/\sigma_0$$

$$A_p = \sigma_p/\sigma_0$$

$$A_{ep} = \sigma_{ep}/\sigma_0$$

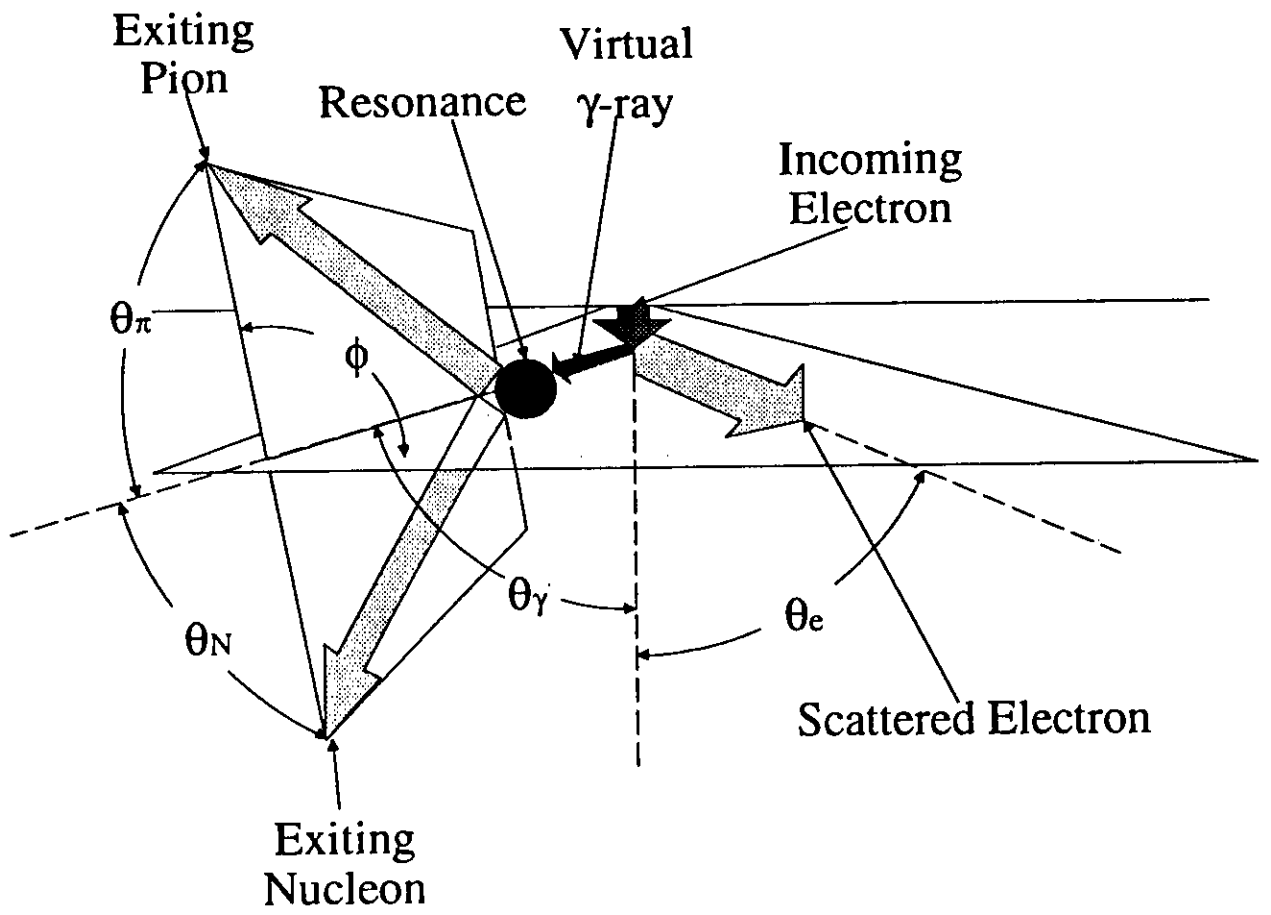


Figure 1

CLAS Acceptance for π^0 Production

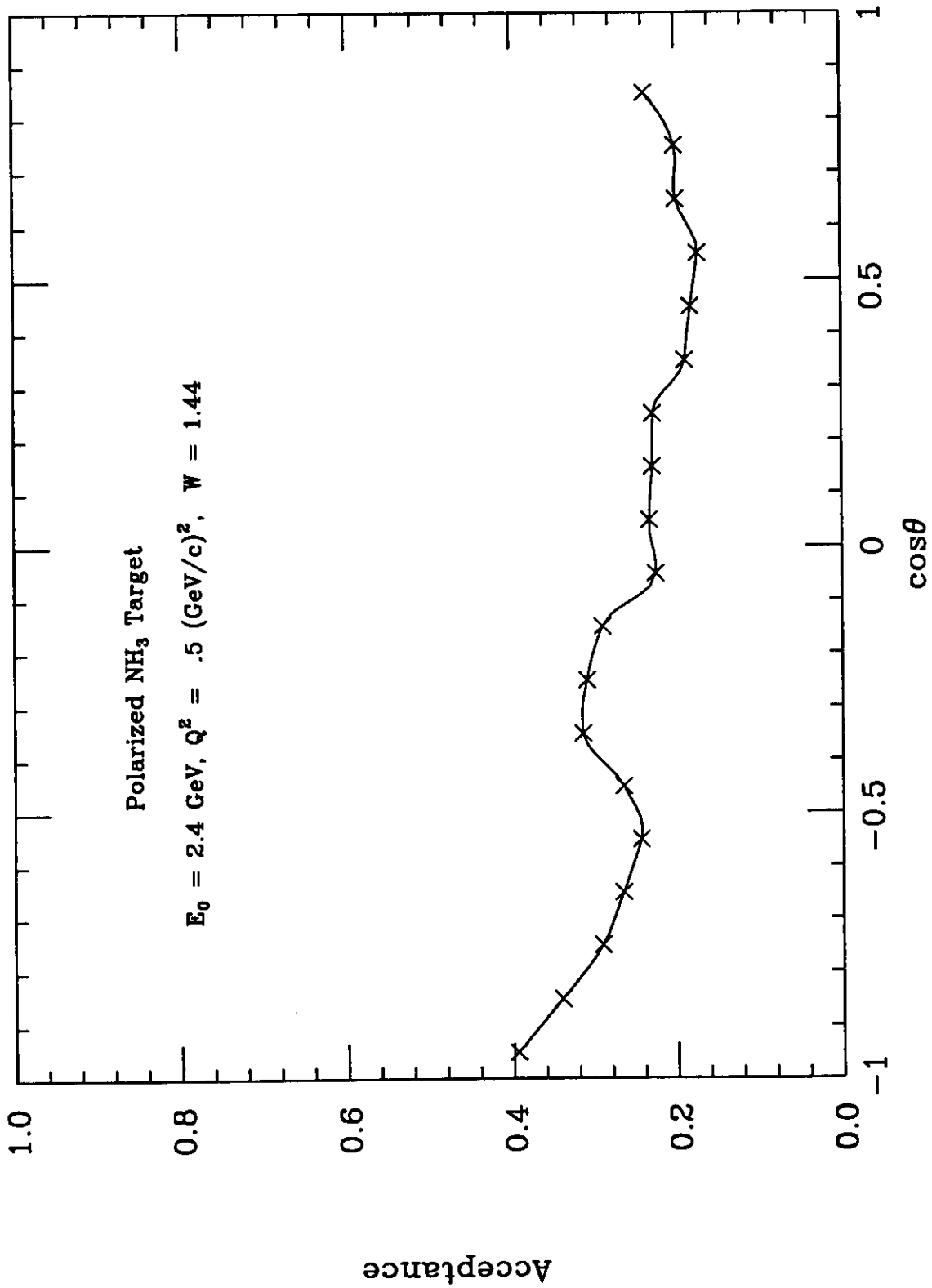
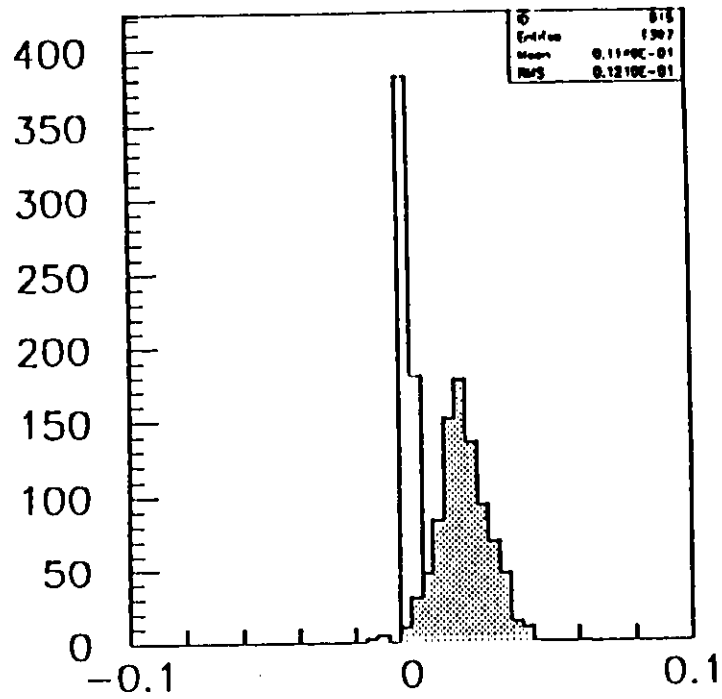
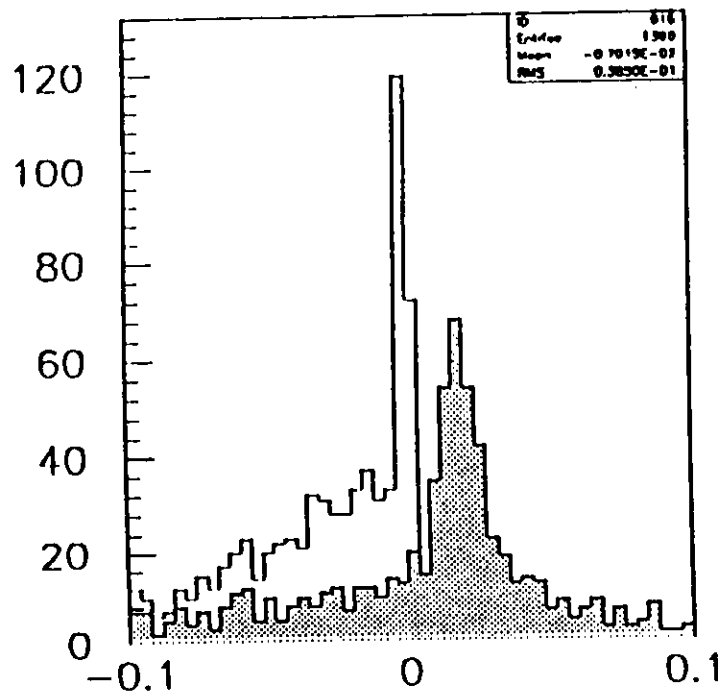
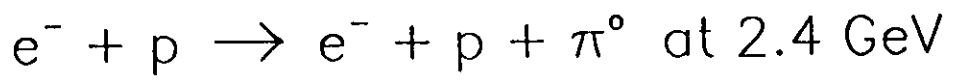


Figure 2



MM2e2



MM2e2

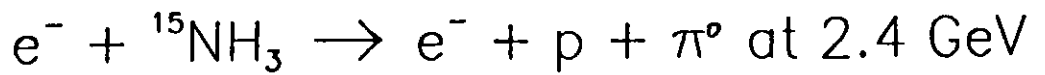
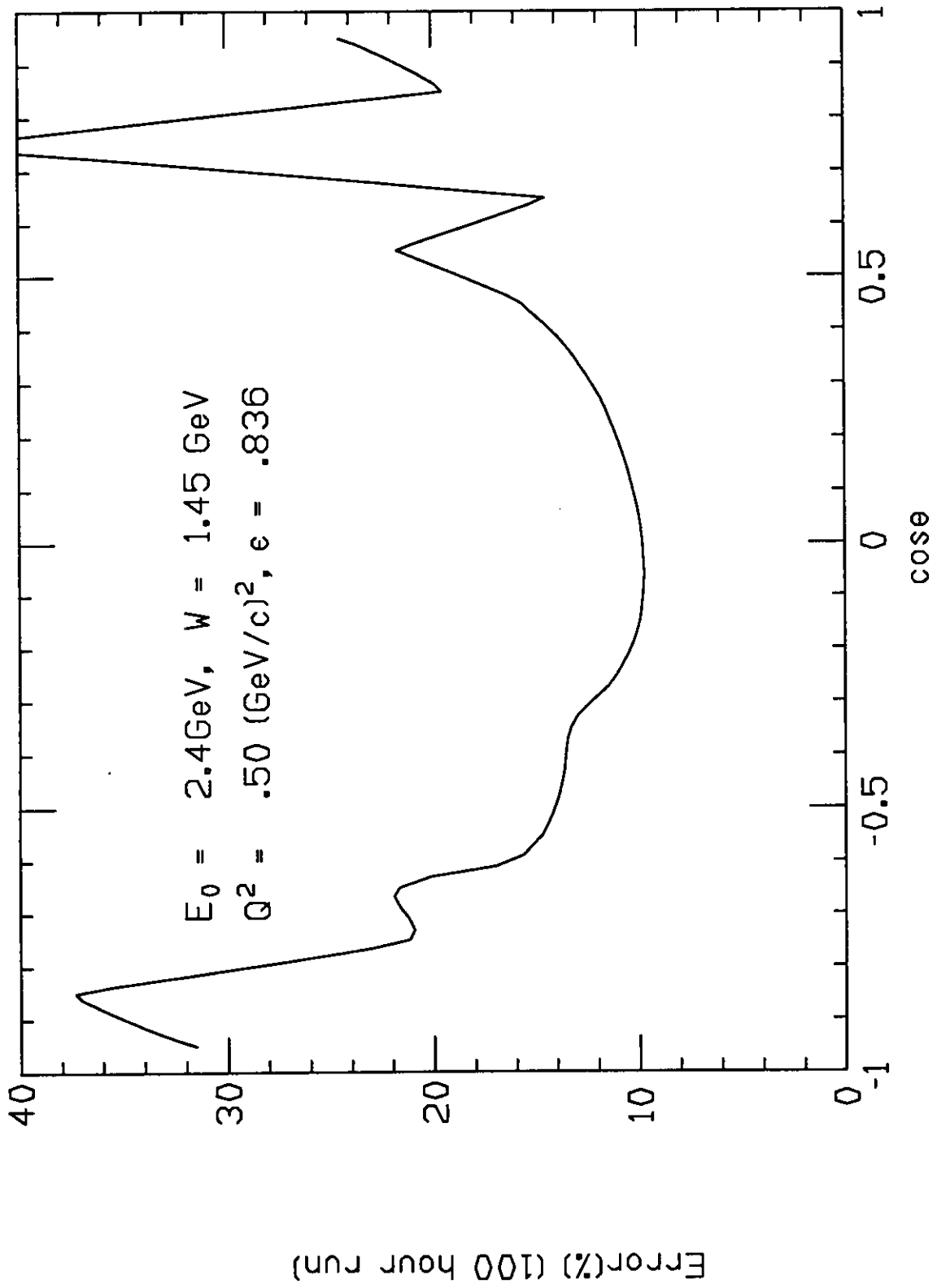


Figure 3

Asymmetry error for π^0 Production



Figure

$P_{11}(1440)$

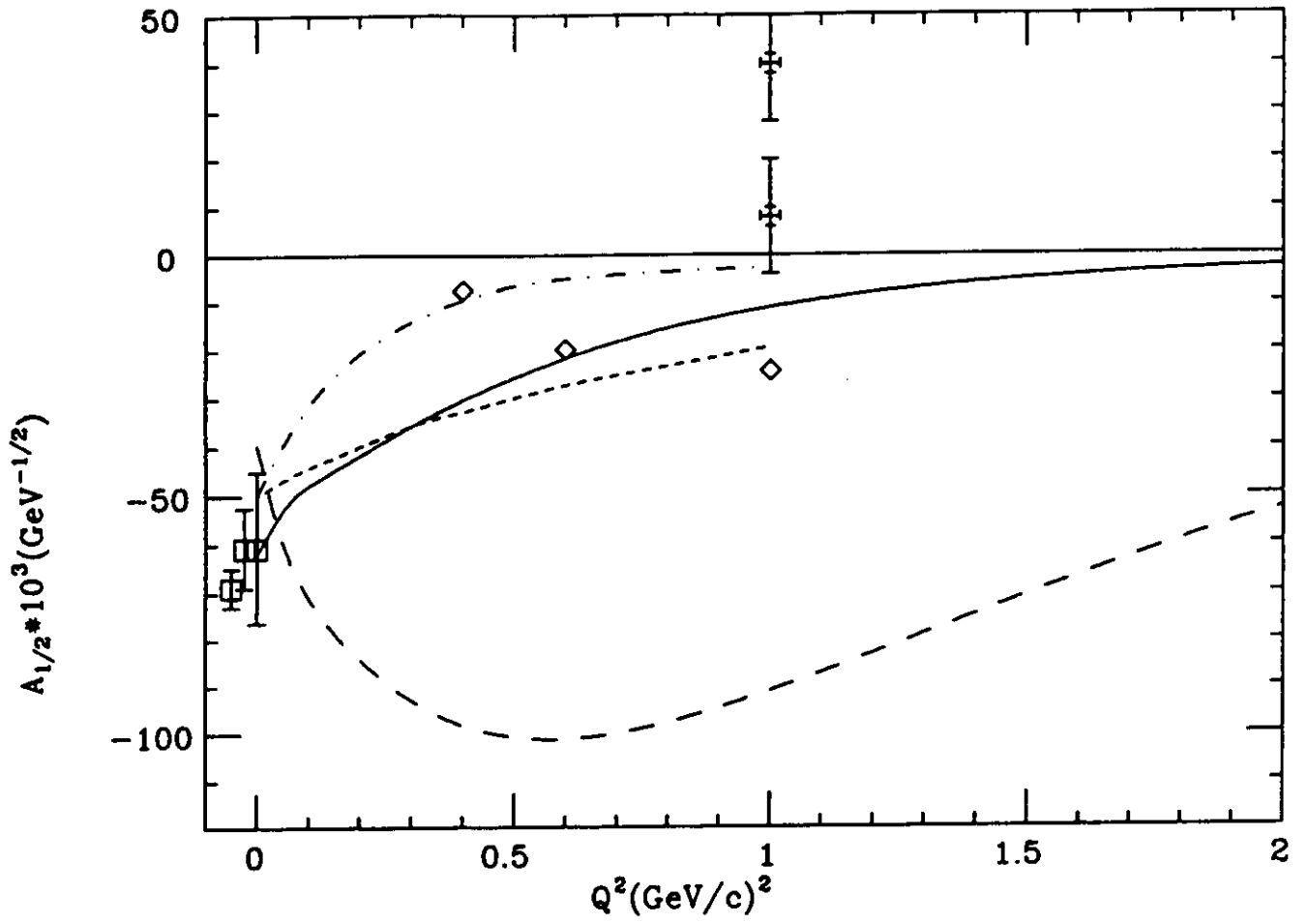


Figure 5

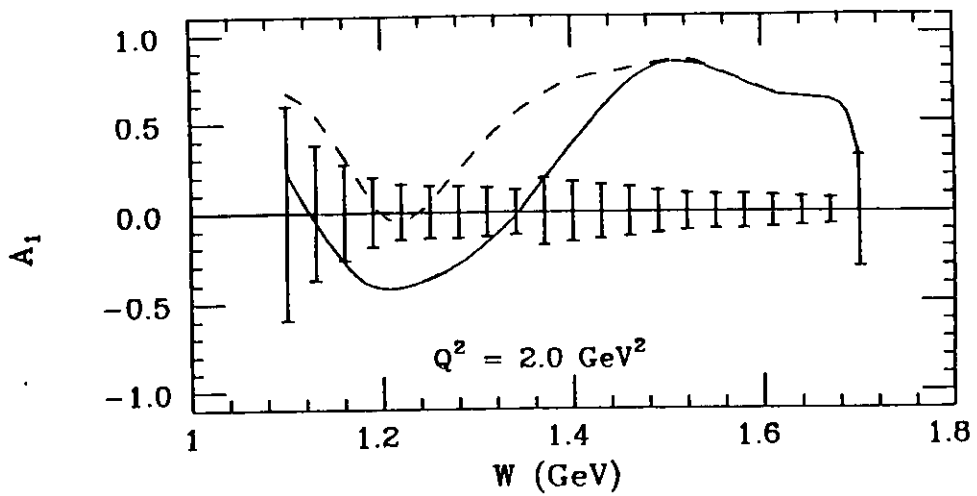
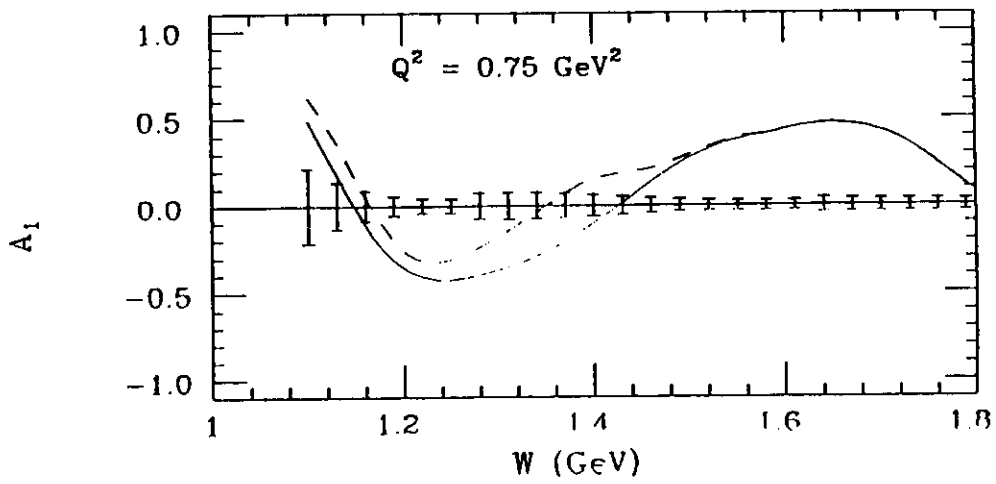
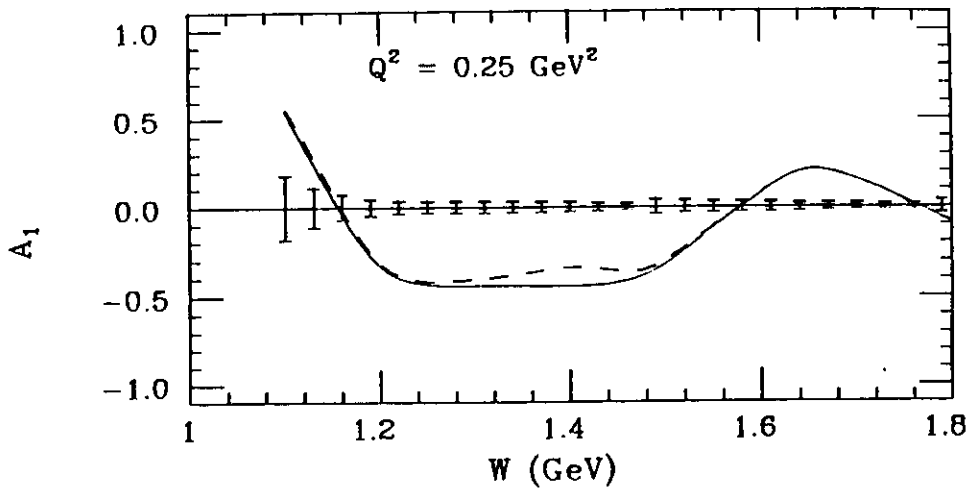
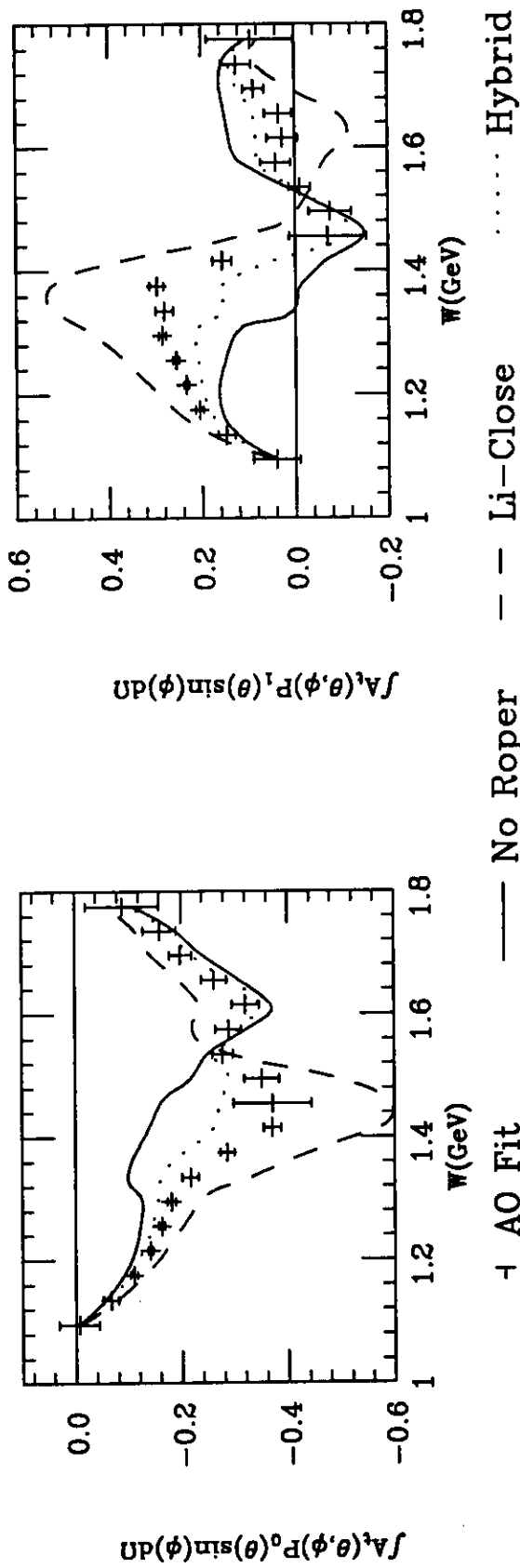


Figure 6

$$\pi^0, E = 2.4, Q^2 = .50 \text{ (GeV/c)}^2$$



$$\pi^0, E = 4.0, Q^2 = 1.50 \text{ (GeV/c)}^2$$

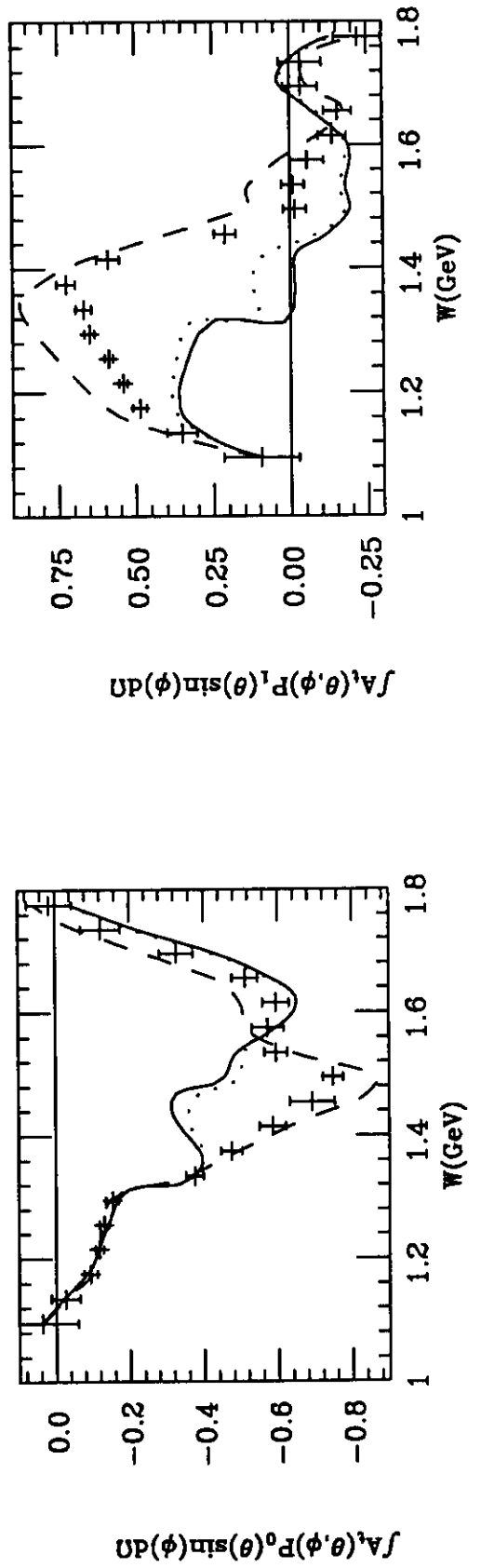
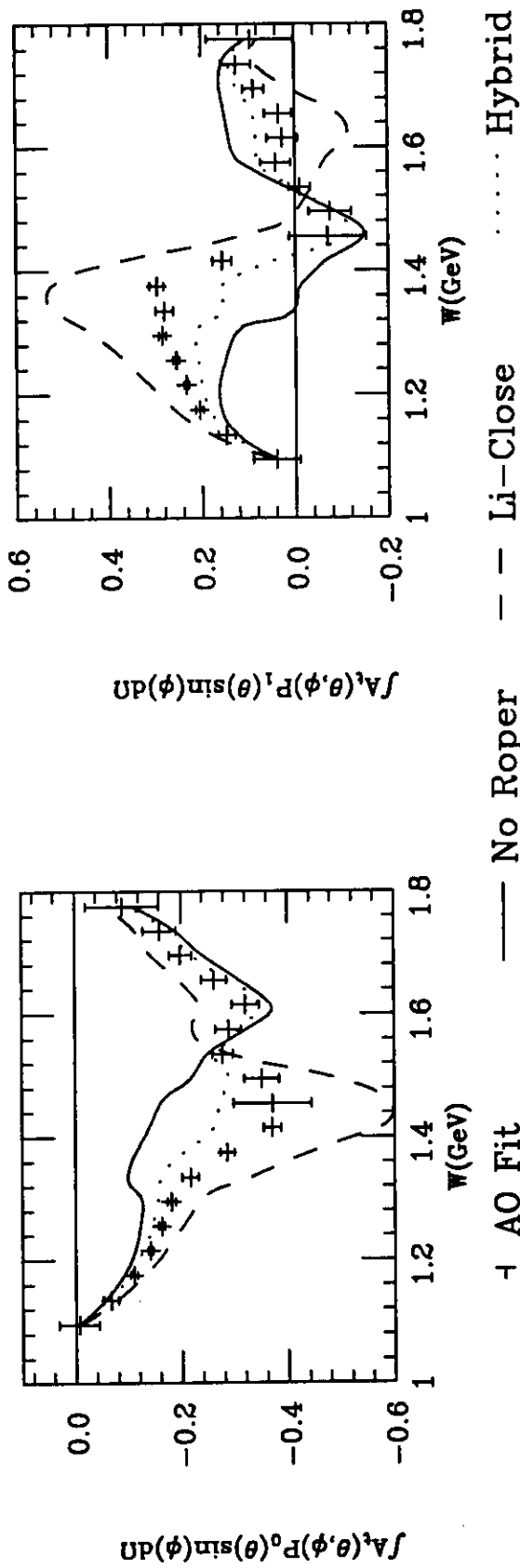


Figure 7

$$\pi^0, E = 2.4, Q^2 = .50 \text{ (GeV/c)}^2$$



$$\pi^0, E = 4.0, Q^2 = 1.50 \text{ (GeV/c)}^2$$

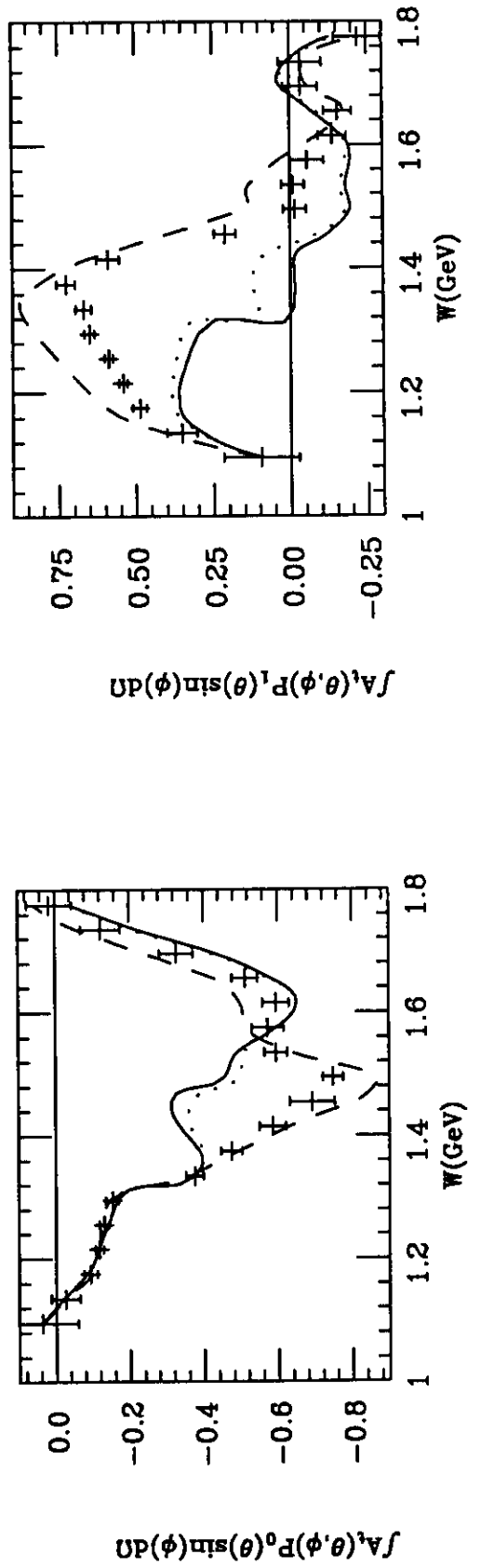


Figure 7

π^+ , $E = 4.0$ GeV, No background

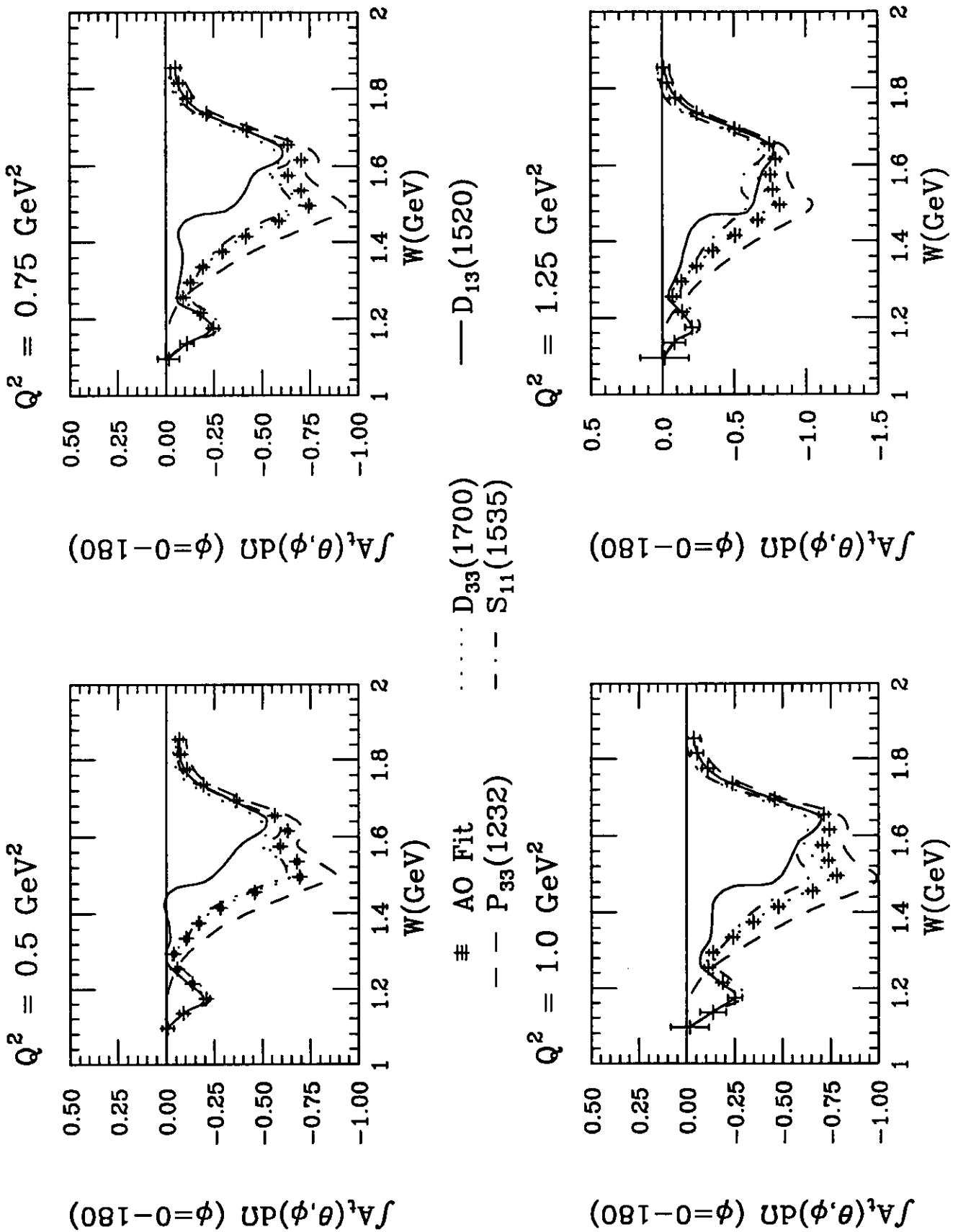
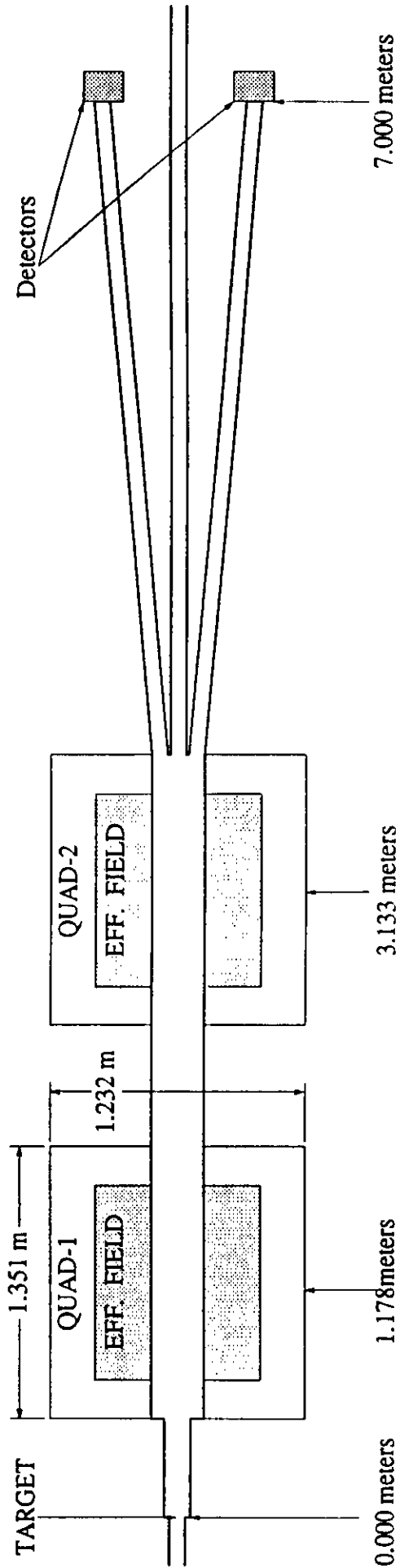


Figure 9



New Hall-B Double Quadrupole Möller Polarimeter

Figure 10

Count Times

- Assume: 1) 100 nA of electron beam.
 2) 1/2 mil Vanadium Permendur target at 20° wrt the beam.
 3) 8% target polarization.
 4) 50% beam polarization.
 5) Want 3% statistical errors.

Times necessary to measure beam polarization within 3% statistical error.

Target	Energy	Long. Time	Trans. Time
N0	700 MeV	16 sec.	12.2 min.
	800 MeV	9 sec.	7.4 min.
	1.0 GeV	11 sec.	8.5 min.
N	1.0 GeV	18 sec.	14.3 min.
	1.6 GeV	20 sec.	15.7 min.
N2	1.6 GeV	17 sec.	13.8 min.
	2.0 GeV	25 sec.	19.4 min.
	2.75 GeV	41 sec.	32.6 min.
N3	2.75 GeV	37 sec.	29.5 min.
	3.0 GeV	44 sec.	35.1 min.
	4.0 GeV	67 sec.	53.1 min.

- For different statistical error multiply times by:
 $(3\%)^2 / (\text{Desired Error})^2$
- Increase in beam intensity or target thickness will decrease measurement time linearly.